

Spectral coherence anomalies

Luyu Wang, Sergey A. Ponomarenko,* and Zhizhang (David) Chen

Department of Electrical and Computer Engineering, Dalhousie University, Halifax, NS B3J 2X4 Canada

*Corresponding author: serpo@dal.ca

Received April 30, 2013; revised June 5, 2013; accepted June 18, 2013;
posted June 19, 2013 (Doc. ID 189770); published July 12, 2013

We describe the anomalous behavior of the spectral degree of coherence as a function of light frequency in the vicinity of phase singularities of partially spatially coherent, polychromatic wave fields. We distinguish the discovered spectral coherence anomalies from conventional spectral anomalies realized with fully spatially coherent optical fields. We also demonstrate how the previously reported spectral anomalies can be engineered in partially spatially coherent fields. © 2013 Optical Society of America

OCIS codes: (030.0030) Coherence and statistical optics; (030.1640) Coherence; (050.1940) Diffraction.

<http://dx.doi.org/10.1364/OL.38.002557>

Singular optics is concerned with the behavior of electromagnetic fields in close proximity to the regions of perfect destructive interference where field amplitudes vanish and, by implication, phases are indeterminate (singular) [1]. Until recently, singular optics dealt, for the most part, with monochromatic, fully spatially coherent scalar [2] or vector [3] fields. In recent years, however, the spectral behavior of focused coherent, polychromatic wavefields in the vicinity of phase singularities was explored and pronounced spectral anomalies were theoretically discovered [4] and experimentally verified [5]. This research was followed by the examination of spectral anomalies in Fraunhofer [6] and Fresnel [7] diffraction of fully coherent light by hard apertures. The discovered spectral anomalies were shown to be generic of fully spatially coherent, polychromatic fields [8].

Concurrently, the behavior of partially spatially coherent, quasi-monochromatic wavefields near phase singularities was also studied, both theoretically [9–15] and experimentally [11,13], and self-similar [10,11] or non-shape-preserving evolution [15–17] of partially coherent singular beams was revealed. Moreover, heuristic arguments were advanced [14] showing that, while phase singularities of field amplitudes are generic to fully spatially coherent fields, so are the correlation function phase singularities to partially spatially coherent fields.

However, it appears that only the anomalous behavior of the spectral intensities of optical fields near their phase singularities has been explored to date. In this Letter, we show that the second-order correlation functions of partially spatially coherent, polychromatic fields also exhibit anomalous spectral features in the vicinity of their phase singularities. We term the novel spectral anomalies the “spectral coherence anomalies” to distinguish them from the previously discussed anomalies of spectral intensities. We note that many realistic light sources, ranging from multimode lasers [18] to light-emitting diodes [19], are partially spatially coherent and polychromatic because they operate at several transverse (spatial) and longitudinal (temporal) modes. Therefore, spectral coherence anomalies are expected to be generic to the fields generated by such sources.

Mathematically, spectral coherence anomalies arise near zeroes of the cross-spectral densities $W(\mathbf{r}_1, \mathbf{r}_2, \omega)$, specifying the second-order statistics of scalar optical field ensembles $\{U(\mathbf{r}, \omega)\}$; $W(\mathbf{r}_1, \mathbf{r}_2, \omega)$ is defined viz. [18],

$$\langle U^*(\mathbf{r}_1, \omega')U(\mathbf{r}_2, \omega) \rangle \equiv W(\mathbf{r}_1, \mathbf{r}_2, \omega)\delta(\omega - \omega'). \quad (1)$$

The angle brackets on the left-hand side of Eq. (1) denote ensemble averaging. As was argued elsewhere [14], spectral anomalies are not ubiquitous in the realm of partially coherent fields whose spectra typically have no zeroes. Hence, spectral coherence anomalies generically occur in the neighborhood of a frequency ω_* in the regions around pairs of points $\mathbf{r}_{1*}, \mathbf{r}_{2*}$ where the spectral degree of coherence of the field, rather than $W(\mathbf{r}_1, \mathbf{r}_2, \omega)$, vanishes, i.e.,

$$\mu(\mathbf{r}_{1*}, \mathbf{r}_{2*}, \omega_*) = 0. \quad (2)$$

Here the spectral degree of coherence is defined as [18,20]

$$\mu(\mathbf{r}_1, \mathbf{r}_2, \omega) = \frac{W(\mathbf{r}_1, \mathbf{r}_2, \omega)}{\sqrt{S(\mathbf{r}_1, \omega)}\sqrt{S(\mathbf{r}_2, \omega)}}, \quad (3)$$

where $S(\mathbf{r}, \omega) \equiv W(\mathbf{r}, \mathbf{r}, \omega)$ is the spectral light intensity.

In this Letter, we will describe the structure of spectral coherence anomalies using a simple, yet illustrative, example. We stress that, although the quantitative features of the presented anomalies depend on the particular (axial) symmetry of the example source, the existence and qualitative features of the discovered spectral coherence anomalies are generic of partially coherent polychromatic optical fields.

To begin, we consider a statistically stationary, broadband coherent light source, a laser oscillating at several longitudinal modes, say, with the spectrum $S^{(i)}(\omega)$, centered at the frequency ω_0 . We can generate a partially spatially coherent secondary source by using a version of the Mach–Zehnder interferometer illustrated in Fig. 1. Conceptually similar setups were employed for the experimental realization of partially coherent beams endowed with optical vortices [11] and polarization singularities [21,22]. An optical path difference greater than the longitudinal coherence length of the primary source can be imposed between the outputs of the beam splitter BS_1 . Consequently, the fields in the two interferometer arms become uncorrelated and the emerging field at the exit to the interferometer is partially spatially coherent. Further, we can place collimating lenses, denoted as

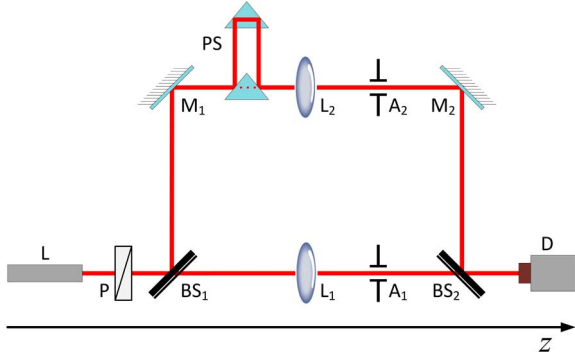


Fig. 1. Partially spatially coherent secondary source. The optical axis of the source is along the z axis.

\mathcal{L}_1 and \mathcal{L}_2 in the figure, in front of the two circular apertures \mathcal{A}_1 and \mathcal{A}_2 with the radii a_1 and a_2 , respectively, to ensure the plane wave input to the apertures. The mirror \mathcal{M}_2 and beam splitter \mathcal{BS}_2 are assumed to be in the far zone of the apertures \mathcal{A}_1 and \mathcal{A}_2 , respectively. Thus, the far-zone spatial field distribution generated in each interferometer arm is given by the well-known Airy diffraction pattern. In this work, we are not interested in light polarization properties. Hence, we can place a polarizer \mathcal{P} in front of the beam splitter \mathcal{BS}_1 to ensure that the output partially coherent field is linearly polarized.

A statistical realization of the far-field output of the interferometer can then be represented within the framework of the scalar theory as

$$U(rs, \omega) \propto \frac{ke^{ikr}}{r} \sum_{p=1,2} c_p(\omega) u_p(\theta, \omega). \quad (4)$$

Here, s is a unit vector in the radial direction, $k = \omega/c$, and θ is the angle that s makes with the optical axis of the system, the z axis. In writing Eq. (4), we assumed that $k_0 a_p \gg 1$, where $k_0 = \omega_0/c$, and the spectral width $\Delta\omega$ is not too large, $\Delta\omega \ll \omega_0$, such that the paraxial approximation, $\sin \theta \simeq \theta$, is appropriate for all frequencies within the bandwidth of $S^{(i)}(\omega)$. The second-order statistics of uncorrelated, statistically stationary spectral amplitudes are specified by

$$\langle c_p^*(\omega') c_q(\omega) \rangle = S^{(i)}(\omega) \delta_{pq} \delta(\omega - \omega'). \quad (5)$$

The angular field distributions in the interferometer arms are given by the paraxial diffraction pattern of a circular aperture [23]

$$u_p(\theta, \omega) = \frac{2J_1(ka_p\theta)}{ka_p\theta}, \quad (6)$$

where $J_1(x)$ is the Bessel function of the first kind and first order.

The cross-spectral density of the secondary source field at the pair of directions s_1 and s_2 on a sphere of radius r in the far zone can be determined from Eqs. (1)–(6) to be

$$W(rs_1, rs_2, \omega) \propto \frac{S^{(i)}(\omega)}{r^2} \left[\frac{G(\theta_1, \theta_2, \omega)}{\theta_1 \theta_2} \right], \quad (7)$$

where we introduced the spectral correlation form-factor as

$$G(\theta_1, \theta_2, \omega) = \sum_{p=1,2} \frac{J_1(ka_p\theta_p) J_1(ka_p\theta_{3-p})}{a_p^2}. \quad (8)$$

We notice that the spectral intensity of the field can be expressed as

$$S(rs, \omega) \equiv W(rs, rs, \omega) \propto \frac{S^{(i)}(\omega)}{r^2} \left[\frac{F(\theta, \omega)}{\theta^2} \right], \quad (9)$$

where the spectrum form-factor is

$$F(\theta, \omega) = \sum_{p=1,2} \frac{J_1^2(ka_p\theta)}{a_p^2}. \quad (10)$$

It follows at once from Eqs. (7) and (9) that

$$\mu(\theta_1, \theta_2, \omega) = \frac{G(\theta_1, \theta_2, \omega)}{\sqrt{F(\theta_1, \omega)} \sqrt{F(\theta_2, \omega)}}. \quad (11)$$

Using Eqs. (8), (10), and (11), the color plot of $|\mu(\theta_1, \theta_2, \omega)|$ is presented in Fig. 2 as a function of the angle θ_2 and frequency ω , for a fixed value of the other angle, $\theta_1 = \bar{\theta}_1$. It is seen in the figure that the spectral degree of coherence changes rapidly in the vicinity of zero-value valleys of $|\mu|$. To confirm the existence of such valleys, we exhibit the frequency evolution of $|\mu(\bar{\theta}_1, \bar{\theta}_2, \omega)|$ in Fig. 3 for the two angular coordinates kept fixed at $\bar{\theta}_1$ and $\bar{\theta}_2$. It can be inferred from Fig. 3 that, given a pair of aperture sizes, there always exists at least one spectral component for which the modulus of the spectral degree of coherence attains zero, indicating

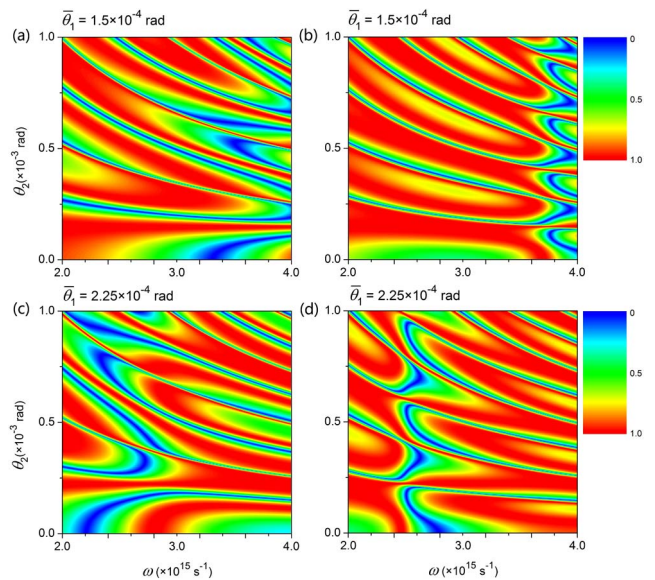


Fig. 2. Magnitude of the spectral degree of coherence as a function of the angle θ_2 and frequency ω . The other angular argument, $\theta_1 = \bar{\theta}_1$, takes on values indicated in the figure. The aperture sizes are: (a) and (c) $a_1 = 2$ mm and $a_2 = 3$ mm; (b) and (d) $a_1 = 2$ mm and $a_2 = 4$ mm.

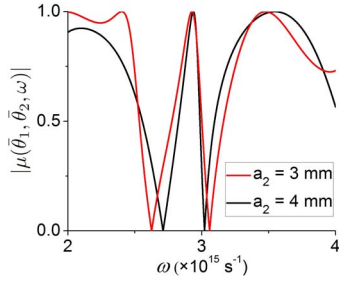


Fig. 3. Frequency evolution of $|\mu(\bar{\theta}_1, \bar{\theta}_2, \omega)|$ for two aperture sizes a_2 , given $a_1 = 2$ mm, $\bar{\theta}_1 = 2.25 \times 10^{-4}$ rad, and $\bar{\theta}_2 = 3.5 \times 10^{-4}$ rad.

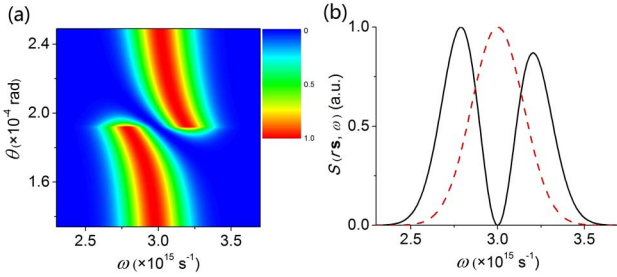


Fig. 4. (a) Engineering a spectral anomaly in the critical direction with $\theta_* = 1.91 \times 10^{-4}$ rad. (b) The secondary source spectral line (black solid line) is split. The primary source spectrum (red dashed line) is a Gaussian.

the presence of a valley. It can also be inferred from Fig. 2 that spectral coherence anomaly locations depend on the parameter values. First, the anomaly locations shift toward lower frequencies as θ_1 increases. Next, for a fixed value of a_1 , the larger a_2 , the more dense the spectral coherence anomaly pattern [compare Figs. 2(a)/2(c) to Figs. 2(b)/2(d)].

Finally, we notice that spectral anomalies of partially coherent fields can be engineered, in our case, by adjusting relative aperture sizes. It follows from Eq. (10) that if, for example, the aperture radii are related as $a_1/a_2 = x_*/x_{**}$, where $x_* \approx 3.83$ and $x_{**} \approx 7.01$ are the first and second zeros of $J_1(x)$, respectively, then the spectrum exhibits the anomalous behavior illustrated in Fig. 4(a). In this case, the primary source spectrum is assumed to be a Gaussian, centered at $\omega_0 = 3.0 \times 10^{15}$ s $^{-1}$ with the linewidth $\Delta\omega = 0.05\omega_0$, while the aperture sizes are $a_1 = 2$ mm and $a_2 = 1.83$ mm. It is seen in Fig. 4(b) that the spectral line is split right in the critical direction, $\theta_* = x_*/k_0a_1 = x_{**}/k_0a_2$.

In conclusion, we mention that spectral switches [6,7], associated with conventional spectral anomalies, found numerous applications ranging from lattice spectroscopy [24] to all-optical digital data transmission [25,26]. By the same token, the discovered spectral coherence anomalies are expected to be useful in optical communications with partially coherent light and spatial coherence spectroscopy, to mention but a few potential applications.

References

1. J. F. Nye, *Natural Focusing and Fine Structure of Light* (IOP, 1999).
2. M. S. Soskin and M. V. Vasnetsov, Vol. 42 of *Progress in Optics*, E. Wolf, ed. (Elsevier, 2001), p. 219.
3. I. Freund, A. I. Mokhun, M. S. Soskin, O. V. Angelsky, and I. I. Mokhun, *Opt. Lett.* **27**, 545 (2002).
4. G. Gbur, T. D. Visser, and E. Wolf, *Phys. Rev. Lett.* **88**, 013901 (2001).
5. G. Popescu and A. Dogariu, *Phys. Rev. Lett.* **88**, 183902 (2002).
6. S. A. Ponomarenko and E. Wolf, *Opt. Lett.* **27**, 1211 (2002).
7. J. T. Foley and E. Wolf, *J. Opt. Soc. Am. A* **19**, 2510 (2002).
8. M. V. Berry, *New. J. Phys.* **6**, 66 (2002).
9. S. A. Ponomarenko and E. Wolf, *Opt. Commun.* **170**, 1 (1999).
10. S. A. Ponomarenko, *J. Opt. Soc. Am. A* **18**, 150 (2001).
11. G. V. Bogatyryova, Ch. V. Felde, P. V. Polyanskii, S. A. Ponomarenko, and E. Wolf, *Opt. Lett.* **28**, 878 (2003).
12. H. F. Schouten, G. Gbur, T. D. Visser, and E. Wolf, *Opt. Lett.* **28**, 968 (2003).
13. D. M. Palacios, I. D. Maleev, A. S. Marathay, and G. A. Swartzlander, *Phys. Rev. Lett.* **92**, 143905 (2004).
14. G. Gbur and T. D. Visser, *Opt. Commun.* **222**, 117 (2003).
15. I. D. Maleev and G. A. Swartzlander, *J. Opt. Soc. Am. B* **25**, 915 (2008).
16. T. van Dijk and T. D. Visser, *J. Opt. Soc. Am. A* **26**, 741 (2009).
17. Y. Yang, M. Mazilu, and K. Dholakia, *Opt. Lett.* **37**, 4949 (2012).
18. L. Mandel and E. Wolf, *Optical Coherence and Quantum Optics* (Cambridge University, 1995).
19. F. Rahman, *Opt. Photon. News* **24**, 26 (2013).
20. S. A. Ponomarenko, H. Roychowdhury, and E. Wolf, *Phys. Lett. A* **345**, 10 (2005).
21. Ch. V. Felde, A. A. Chernyshov, G. V. Bogatyryova, P. V. Polyanskii, and M. S. Soskin, *JETP Lett.* **88**, 418 (2008).
22. A. A. Chernyshov, Ch. V. Felde, G. V. Bogatyryova, P. V. Polyanskii, and M. S. Soskin, *J. Opt. A* **11**, 094010 (2009).
23. M. Born and E. Wolf, *Principles of Optics*, 7th ed. (Cambridge University, 1999).
24. P. Han, *Opt. Lett.* **34**, 1303 (2009).
25. J. Pu, C. Cai, and S. Nemoto, *Opt. Express* **12**, 5131 (2004).
26. P. Han, *Opt. Lett.* **37**, 2319 (2012).